

Adsorption of cationic and anionic organic dyes on SiO₂/CuO composite

Mahmoud Sunjuk^a, Husam Arar^b, Wadah F. Mahmoud^c, Majdi Majdalawi^b,
Monzer M. Krishan^d, Yousef Abu Salha^c, Bassam El-Eswed^{b,*}

^aChemistry Department, Faculty of Science, The Hashemite University, Zarqa, Jordan, email: Mahmoud.Sunjuk@hu.edu.jo

^bZarqa College, Al-Balqa Applied University, P.O. Box: 313, Zarqa 13110, Jordan, emails: bassameswed@bau.edu.jo (B. El-Eswed), husamarar@yahoo.com (H. Arar)

^cGeology Department, The University of Jordan, Amman 11942, Jordan, emails: w.mahmoud@ju.edu.jo (W.F. Mahmoud), abusahayama@yahoo.com (Y.A. Salha)

^dDepartment of Mechatronics Engineering, Al-Balqa Applied University, Amman 11134, Jordan, email: drkrishan@bau.edu.jo (M.M. Krishan)

Received 27 January 2019; Accepted 13 July 2019

ABSTRACT

Silica (SiO₂) is one of the most abundant minerals in soils and sediments. Copper oxide (CuO) is a low-cost material with an excellent antimicrobial property. In the present work, a composite comprising silica and copper oxide (SiO₂/CuO) was synthesized by dissolution of SiO₂ (cristobalite) in 6.0 M NaOH followed by deposition of dissolved SiO₂ on CuO. The composite was characterized using XRF, XRD, SEM and FTIR techniques. The XRF analysis indicated that SiO₂/CuO contains 79.42 wt% CuO and 14.36 wt% SiO₂. Both XRD and SEM analysis revealed that silica exists in SiO₂/CuO as amorphous agglomerates. The Si–O–Si stretching at 1,076 cm⁻¹ in the FTIR spectrum of SiO₂ was shifted to 1,033 cm⁻¹ in the case of SiO₂/CuO due to dissolution of SiO₂ and interaction with CuO. Two types of organic dyes, namely, cationic (methylene blue [MB], crystal violet [CV]) and anionic dyes (acid blue 29 [AB], Congo red [CR]) were tested for their adsorption on SiO₂/CuO which was found to have much more dye adsorption capacity than the precursors (SiO₂ and CuO). Furthermore, SiO₂/CuO had an exceptional fast rate of adsorption for the MB and CV where 77% and 66% of the initial amounts were removed within 1 min, respectively. On the other hand, the anionic dyes were found to be poorly adsorbed on SiO₂/CuO. However, when ionic strength increased from 0.0 to 0.5 M NaCl, the adsorption of anionic dyes such as CR increased from 0.4% to 82.3%, while the adsorption of cationic dyes such as MB decreased from 91% to 28%. Thus, the selective removal of dyes can be achieved by controlling the ionic strength.

Keywords: Adsorption; Copper oxide; Silica; Cristobalite; Methylene blue; Crystal violet; Acid blue; Congo red

1. Introduction

Preparation of composite adsorbent is a potential approach to modify the adsorption behavior of original materials without losing their advantages. Inorganic composites have high temperature stability, long shelf life and resistance to environmental and biological conditions. A silica–copper oxide composite is the topic of the present study.

Silica is an important mineral in earth's crust with abundance of about 12% [1]. Crystalline silica polymorphs, such as α -quartz and α -cristobalite are the most abundant silicate minerals species in soils and sediments. Furthermore, α -cristobalite usually occurs in the dust falls of the ceramics industry [2]. Cristobalite (diatomaceous earth celite 545) is selected as a source for SiO₂ in the present work because it is more soluble than quartz in alkaline solutions [3].

* Corresponding author.

Tsai et al. [4] reported that alkaline etching of diatomaceous earth in 2 M NaOH at 100°C for 2 h gives a mesoporous amorphous silicate material.

Copper oxide-based materials have destructive effect on bacteria, viruses, algae, protozoa and fungus [5,6] with a significant activity against gram positive and negative bacterial strains. They are more stable under high temperature and have longer shelf lives than organic-based antimicrobial materials [7,8].

Organic dyes are widely used in textile, paper, plastic, carpets and printing industries [9]. More than 7×10^5 tonnes of dyes are produced annually, and about 2% of this amount of dyes is discharged into wastewater [10]. The presence of color in the aquatic media reduces the penetration of sunlight to the benthic organisms, thus limiting the process of photosynthesis. Despite these environmental problems, dyes and their metabolites are thought to be mutagens and carcinogens [11]. Dyes can be divided into cationic and anionic dyes depending on their charge developed upon dissolution in aqueous solution [9].

Different types of adsorbents for dyes were reviewed in the literature such as activated carbon [9,12], clay [9,13], zeolites [9,14,15], metal oxides [9], geopolymers (alkali activated aluminosilicates) [16,17], industrial by-products (metal hydroxide sludge, coal fly ash and red mud) [9], agricultural waste (wheat bran, orange peel, rice husk, etc.) [9,10,18] and biosorbents (chitin, chitosan, peat, etc.) [9].

Silicates have received little attention as adsorbents for organic dyes. However, they are potential adsorbents because of their low cost, availability, readiness to modification, mechanical stability and high surface area [9]. Allingham et al. [19] found that the rate of adsorption of cationic dyes such as methylene blue (MB) and crystal violet (CV) on silica (commercial silica dust, vitreous silica, quartz) is very high and reaches equilibrium in few minutes, indicating that the adsorption is taking place on the external surface of the silica powders. On the other hand, the adsorption rate of anionic dyes such as Orange I and II on silica was found to be much lower than that of cationic dyes [19]. Chakrabarti and Dutta [20] studied the adsorption of methylene blue on glass fibers (glass wool); the adsorption capacity (Q_m) and the affinity constant (K_L) were 2.24 mg/g and 0.17 L/mg, respectively. The adsorption capacity of methylene blue on α -quartz and α -cristobalite was reported to be 0.996 and 0.724 mg/g, respectively [2]. Thus, despite the advantage of fast adsorption of organic dyes on silicates, the adsorption capacity is low.

In order to improve their interaction with organic dyes, the surfaces of silicates were modified using amino-silane coupling agents [21]. Furthermore, silica gel was modified by coupling of sodium silicate with titanium and magnesium oxides in the presence of acid activator. The adsorption capacity of acid blue 40 on silica-titania gel and silica-titania-magnesium gel was 17.5 and 9.3 mg/g, respectively [22].

The adsorption capacities of basic violet and basic red on CuO nanoparticles were found to be 16.86 and 27.24 mg/g, respectively, but the Langmuir affinity constant were very low (0.00143 and 0.0084 L/mg, respectively) [23]. CuO nanoparticles were used as catalysts for photo-degradation of organic dyes [24,25].

The aim of the present article is to prepare and characterize a composite from silica and copper oxide. The

adsorption behavior of cationic dyes (methylene blue and crystal violet) and anionic dyes (acid blue 29 and Congo red) on the composite will be studied.

2. Experimental

2.1. Materials

Diatomaceous earth (SiO_2 , celite 545) was obtained from Sigma-Aldrich (Germany) and its XRD pattern (Fig. 1a) showed that the main composition is cristobalite [26]. Copper (II) oxide was purchased from Riedel-de Haen (Germany). Sodium hydroxide and hydrochloric acid solution (35%) were supplied from VWR BDH Chemicals and GCC (UAE). Methylene blue (MB) and crystal violet (CV) were obtained from UNICHEM (India) and GCC (UAE), respectively. Acid blue 29 (AB) and Congo red (CR) were purchased from Sigma-Aldrich (Germany).

2.2. Preparation of SiO_2/CuO composite

A 25.0 g of CuO and 25.0 g of diatomaceous earth (SiO_2) were mixed with 100.0 mL of 6.0 M NaOH solution in plastic container, using plastic spatula. The immediately formed paste was then placed in an oven (Memmert UF 75, Germany) for 24 h at 70°C, and then mixed with 2.0 L of deionized water and the produced solid was filtered off using filter paper and washed with wt.% HCl solution followed by distilled water. The obtained gray solid SiO_2/CuO solid was dried in the oven at 60°C to obtain very fine solid particles. The absence of blue color (Cu(II) ions in the filtrate indicated that CuO remained insoluble throughout the preparation process.

2.3. Characterization of SiO_2/CuO

The FTIR spectra were obtained using Vertex 70 Bruker (Germany) FTIR spectrometer. The XRF analysis was carried out using Shimadzu XRF-1800 instrument. FEI inspect F50 scanning electron microscope was used to record the SEM micrographs of the particles after coating with platinum. The XRD patterns were recorded using X-ray diffractometer (Shimadzu XRD-7000, Japan) equipped with Cu $K\alpha$ radiation source, an Ni filter operating at 40kV/30 mA in the range $2^\circ \leq 2\theta \leq 60^\circ$ with scanning speed of $2^\circ/\text{min}$. Scherrer's Formula ($D = K \lambda / (\beta \cos \theta)$) was used to calculate the crystallite size, where D is the average crystallite size (nm), K is the Scherrer constant which equals 0.94, λ is the X-ray wavelength which is 1.54178 Å for Cu $K\alpha$, β is the full width at half maximum of XRD peak, and θ is the XRD peak position (one half of 2θ) [27].

Potentiometric titration of 0.50 g of SiO_2/CuO in 100.0 mL deionized water with 0.013 M NaOH or HCl was carried out using Hanna (USA) (HI 2212) pH meter. Similar titrations were also done on 100.0 mL deionized to obtain reference pH titration curves. The pH of the point of zero charge (pH_{pzc}), which is defined as the pH at which the charge on the surface of SiO_2/CuO is zero, was determined by the pH drift method. [28]. The initial pH (pH_i) of test solutions (20 mL of 0.01 M NaCl in a series of Erlenmeyer flasks) was adjusted in the pH range between 2 and 11 by adding NaOH or HCl. After that, 0.20 g sample of SiO_2/CuO was added

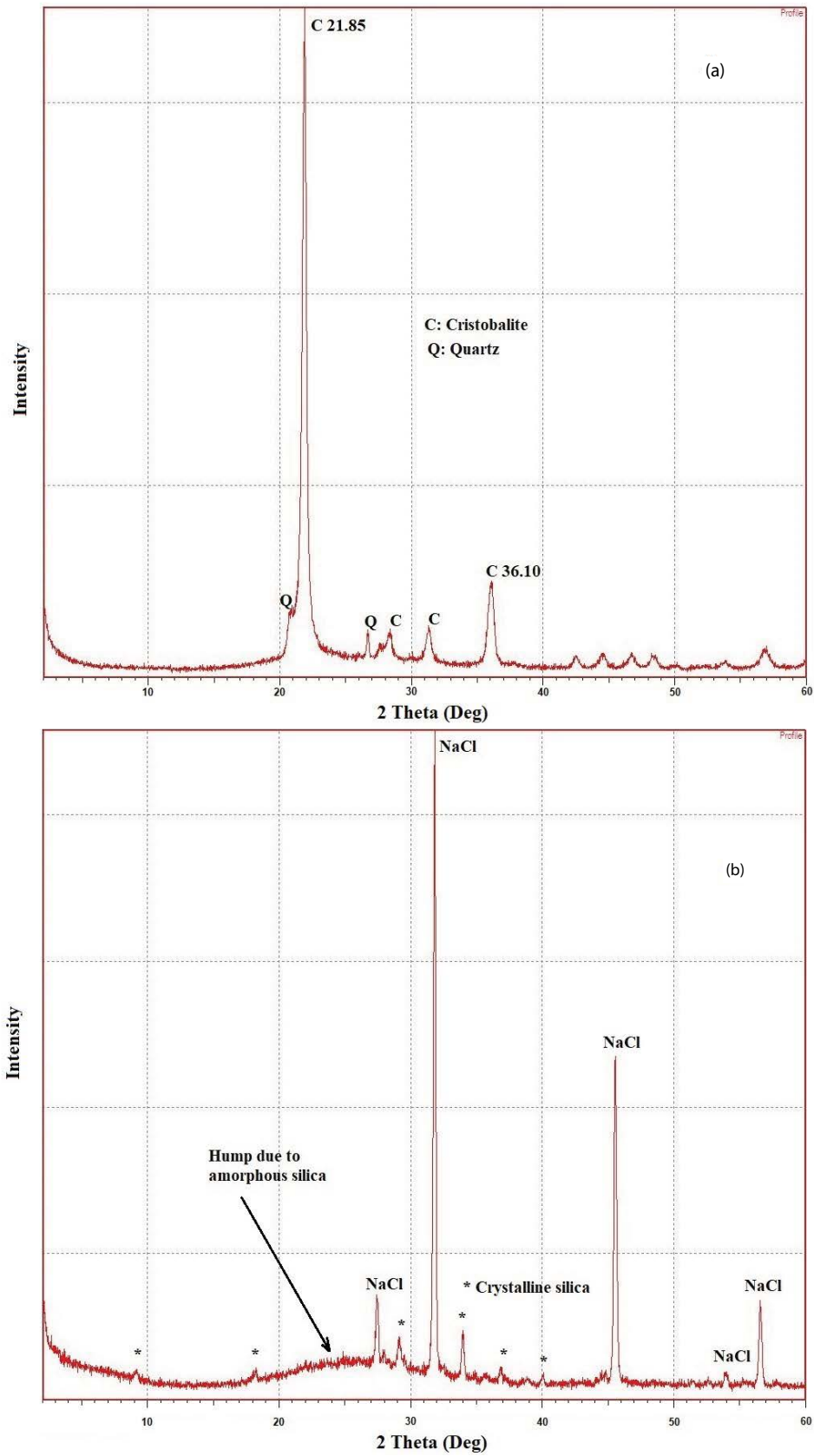


Fig. 1. XRD pattern of (a) diatomaceous earth (SiO_2) and (b) silica gel formed as a result of neutralization of dissolved SiO_2 in 6.0 M NaOH. Assignment of peaks was according to the study by Su et al. [35].

and the final pH (pH_f) was measured after shaking for 24 h. The difference between pH_i and pH_f was plotted against pH_i and the pH_{pzc} was taken as that at which the difference is zero. The pH_{pzc} of CuO and SiO_2 was also determined for the purpose of comparison.

2.4. Adsorption experiments

Batch adsorption studies of the organic dyes on SiO_2/CuO were performed by agitating 25.0 mL of the dye's solutions (MB, CV, AB and CR) of various concentrations (C_i) with 0.20 g of SiO_2/CuO in a shaker (Kushner, Switzerland) at 25°C and 140 rpm for 24 h. After filtration, the concentration of the dye remained in solution (C_e) was determined by UV/Visible spectrophotometer (SP UV-19 SCO Tech) at 650, 590, 602 and 497 nm, respectively. The amount of the dye adsorbed on SiO_2/CuO (Q_e , mg/g) was calculated from the difference between the initial (C_i , mg/L) and equilibrium (C_e , mg/L) dye concentration in solution according to Eq. (1):

$$Q_e = \frac{C_i - C_e}{m} V \quad (1)$$

where V is the volume of solution (L), and m is the mass of SiO_2/CuO (g).

In order to study the effect of contact time on the adsorption of dyes on SiO_2/CuO , aliquots of 25.0 mL of 20 ppm dye solutions were added to 0.5 g SiO_2/CuO . The solution was then shaken for different periods of time (1–1,680 min) at a temperature of 25°C. At specific time, 2.0 mL of the solution was withdrawn to a cuvette using micropipette to measure its light absorbance and then it was returned to the mother solution.

2.5. Models used for fitting adsorption data

2.5.1. Adsorption kinetics

Several kinetic models were used to fit the kinetics data, namely, pseudo-first-order and pseudo-second order, Weber–Morris intraparticle diffusion and linear film diffusion models [29]. Only pseudo-second order model (Eq. (2)) gives satisfactory fitting.

$$\frac{dQ_t}{dt} = k_2(Q_e - Q_t)^2 \quad (2)$$

where Q_t and Q_e are the quantities of dye adsorbed at time t and equilibrium time, respectively and k_2 is the second order rate constant ($\text{g mg}^{-1} \text{min}^{-1}$). Integrating Eq. (2) with initial conditions of $Q_t = 0$ when $t = 0$ and subsequent rearrangement gives the linearized form:

$$\frac{t}{Q_t} = \frac{1}{k_2 Q_e^2} + \frac{t}{Q_e} \quad (3)$$

A plot of $\frac{t}{Q_t}$ vs. t gives a line with a slope = $\frac{1}{Q_e}$ and an intercept = $\frac{1}{k_2 Q_e^2}$ [29].

2.5.2. Adsorption isotherms

Langmuir (Eq. (4)) and Freundlich (Eq. (5)) models were used to fit the adsorption isotherms:

$$Q_e = \frac{Q_m K_L C_e}{1 + (K_L C_e)} \quad (4)$$

$$Q_e = K_F C_e^{1/n} \quad (5)$$

where Q_m (mg/g) is the maximum adsorption capacity, and K_L (L/mg) is the affinity constant of the adsorbate toward the adsorbent. K_F is the Freundlich constant which is an indicator of adsorption capacity and $1/n$ is a measure of adsorption intensity. Both K_F and $1/n$ are system specific constants [30].

3. Results and discussion

3.1. Preparation and characterization of SiO_2/CuO

This work developed a simple method for preparation of SiO_2/CuO composite from silica (SiO_2 , diatomaceous earth composed of cristobalite) and copper oxide (CuO) in the presence of 6.0 M NaOH solution. This method was based on dissolution of silica and its subsequent deposition on CuO particles. Langston and Jenne [31] reported that 12.1% of cristobalite is dissolved upon boiling with 2.0 M NaOH for 24 h (0.1 g cristobalite: 100 mL NaOH solution). In the present work, 81.7% of silica was dissolved in 6.0 M NaOH (boiling 5.0 g cristobalite in 20.0 mL of 6.0 M NaOH solution for 2 h). The dissolved silica was transformed into colorless silicate gel by neutralization with diluted HCl. The XRD of the formed silica gel (Fig. 1b) showed a broad diffracted peak due to amorphous silica phase and small peaks of crystalline phases. Typical peaks of NaCl which results from neutralizing the basic solution with HCl were also observed.

3.2. Characterization of SiO_2/CuO

3.2.1. FTIR study

The FTIR spectra of SiO_2 and SiO_2/CuO are shown in Fig. 2. The Si–O–H stretching vibrations, which are usually observed at 3,250–3,450 cm^{-1} and 960–975 cm^{-1} in silicates materials [32,33], were not observed in the FTIR spectra of SiO_2 and SiO_2/CuO . Their absence in the case of SiO_2 is due to the fact that the commercial diatomaceous earth used in this work was subjected to calcination in manufacturing. The absence of O–H stretching band in the FTIR spectrum of SiO_2/CuO indicates that there is no Si–OH, Cu–OH or H_2O in the composite.

The strong absorption band of Si–O–Si stretching at 1,076 cm^{-1} [34] in the FTIR spectrum of SiO_2 was shifted slightly to lower frequency at 1,067 and 1,033 cm^{-1} in the spectrum of SiO_2/CuO . The other two characteristics bands of Si–O–Si at 792 and 468 cm^{-1} [35,36] in the spectrum of SiO_2 were observed at 794 and 470 cm^{-1} , respectively, (without significant shift) in the spectrum of SiO_2/CuO . The presence of band 1,631 cm^{-1} in the spectrum of SiO_2/CuO is due to stretching vibration of Cu–O [37].

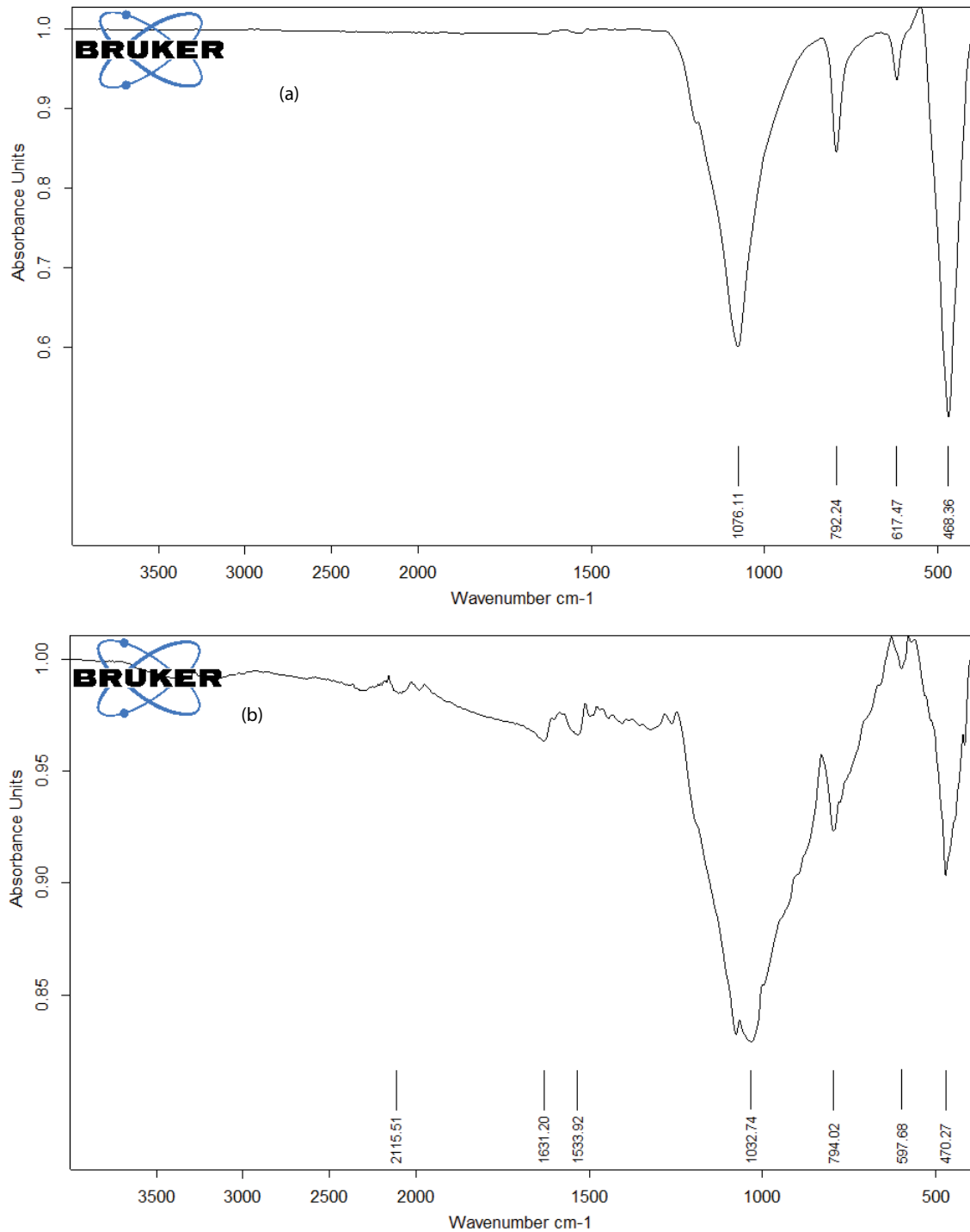


Fig. 2. FTIR spectra of (a) diatomaceous earth (SiO₂) and (b) SiO₂/CuO.

Su et al. [35] reported that deposition of SiO₂ on Cu₂O resulted in a new bond of Cu–O–Si at the interface between the two materials. The Cu–O–Si bond changes the bond strain of Si–O–Si and causes disorder or deformation of SiO₂ framework and consequently new FTIR bands were observed at 1,236 cm⁻¹ [35] and 1,203 cm⁻¹ [36]. Thus, the weak bands in the range from 1,250 to 1,200 cm⁻¹, which were observed in the spectrum of SiO₂/CuO (Fig. 2), may be due to this effect.

3.2.2. XRF analysis

The results of XRF analysis for SiO₂/CuO are given in Table 1. The major components of the composite are CuO (79.42%) and SiO₂ (14.36%). The relatively low SiO₂ to CuO ratio suggests that CuO particles are coated with a layer of SiO₂. Interestingly, the amount of Na in SiO₂/CuO was negligible, although the amount of NaOH used in its preparation

Table 1
Chemical composition of SiO₂/CuO composite

CuO	79.42
SiO ₂	14.36
Al ₂ O ₃	3.41
MgO	1.41
Fe ₂ O ₃	0.89
CaO	0.43
K ₂ O	0.072

was relatively large. This observation excludes the possibility of existences of nonbridging >SiO⁻Na⁺ in SiO₂/CuO. Consequently, formation of polymeric silica on the surface of CuO may be a more plausible hypothesis.

3.2.3. XRD study

The XRD patterns of CuO and SiO₂/CuO are presented in Fig. 3. Both CuO and SiO₂/CuO exhibited the typical XRD pattern of tenorite (CuO) [7]. The reported characteristic peaks of tenorite are (2θ (Intensity)): 35.60(1), 38.78(0.96) and 35.45(0.49) [38]. Using the Scherrer formula, the calculated crystallite size (*D*) of CuO and SiO₂/CuO were 32 and 29 nm, respectively (Table 2). The ionic size of Si(IV) is 40 pm, which is lower than that of Cu(II), which is 87 pm [39]. Thus, Si(IV) may replace some of Cu(II) of CuO in the composite. The XRD peaks of SiO₂ (cristobalite, Fig. 1a) at 2θ = 21.85 and 36.10 disappeared in SiO₂/CuO (Fig. 3) indicating the loss of crystallinity of silica. However, a new weak broad band at 2θ = 21.68 (4.096 Å) was observed in SiO₂/CuO which is due to the formation of amorphous silica in SiO₂/CuO. Similar XRD broad peaks at 2θ = 22–23 were observed in the case of amorphous silica obtained from thermal [36] and alkali treatment [37] of rice hulls.

3.2.4. SEM study

The SEM of SiO₂/CuO showed agglomerated micro-particles (Fig. 4a). Amorphous silica (fate color) and crystalline CuO (brittle color) were observed in the composite (Figs. 4b–d), where the amorphous silica and CuO were amalgamated with each other. The morphology of silica in SiO₂/CuO was similar to that of the amorphous silica obtained from rice husk ash and bagasse ash [40–42].

3.2.5. pH titration curve and point of zero charge

The pH titration curves of SiO₂/CuO (Fig. 5a and b) with NaOH and HCl were found to be very close to the pH titration curve of blank water. Thus, small amounts of acidic Si-OH or basic Si-O⁻ groups are present in SiO₂/CuO.

Fig. 5c illustrates the plot obtained from the pH drift method. From the graph, the pH_{pzc} values obtained for SiO₂/CuO, CuO and SiO₂ were 6.30, 6.95 and 7.10, respectively. Thus, in agreement of the results of the pH titration curve, few amounts of acidic Si-OH groups may be present on the surface of SiO₂/CuO.

3.3. Adsorption of organic dyes on SiO₂/CuO

3.3.1. Comparison of the composite with precursors

The % uptake (amount adsorbed/initial amount) of MB and CV by SiO₂/CuO was compared with those of the precursors (CuO and SiO₂) in Fig. 6. The composite was found to be more effective than CuO and SiO₂ for adsorption of dyes.

Interestingly, alkali-treated SiO₂ in the absence of CuO and alkali-treated CuO in the absence of SiO₂ were much less effective for adsorption of dyes than SiO₂/CuO (Fig. 6). This indicated the importance of the conjunction of SiO₂ and CuO in the composite. The formation of Cu–O–Si bonds at

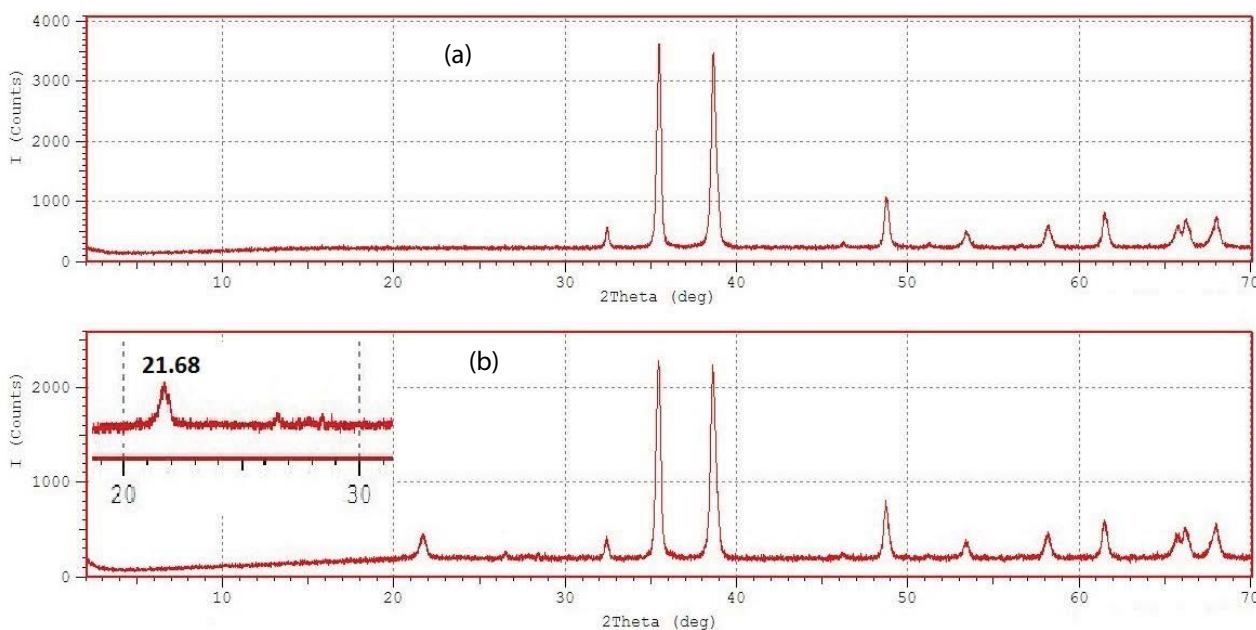


Fig. 3. XRD patterns of (a) CuO and (b) SiO₂/CuO.

Table 2
Average crystallite size of CuO and SiO₂/CuO composite

CuO			SiO ₂ /CuO		
Peak position (2θ)	β	D (nm)	Peak position (2θ)	β	D (nm)
35.4496	0.2804	31.09	35.4164	0.3058	28.50
38.6333	0.2893	30.42	38.609	0.3474	25.33
48.7352	0.2768	32.93	48.7024	0.2975	30.64
58.149	0.358	26.54	53.3587	0.3475	26.74
61.4852	0.2596	37.22	58.127	0.3641	26.09
D average (nm)		31.64	D average (nm)		29.55

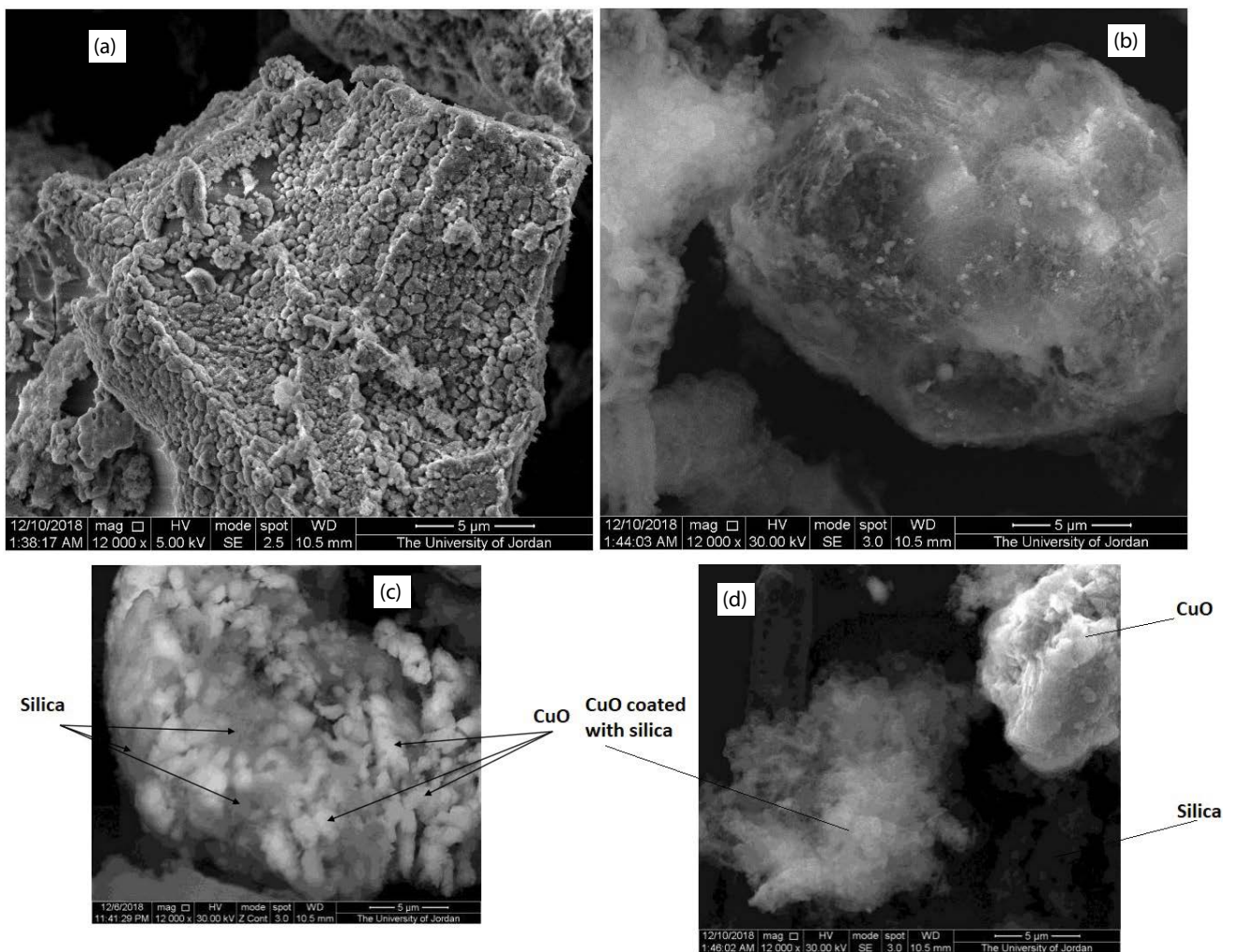


Fig. 4. SEM graph of SiO₂/CuO (a and b), backscattered image (c), and secondary electron image (d).

the interface between SiO₂ and CuO was reflected by the FTIR study (section 3.2.1). The formation of these bonds changes the bond strain of Si–O–Si and thus resulting in an increase of disorder in the SiO₂ network that deposited on CuO in the composite [35]. These changes induced by interaction of CuO with SiO₂ may be responsible for the adsorption of MB and CV.

3.3.2. Kinetics of adsorption

The effect of contact time on the adsorption of MB and CV onto SiO₂/CuO is shown in Fig. 7. The kinetic study showed that 77% of MB and 66% of CV were adsorbed within 1 min, which indicated that the adsorption process is extremely fast. However, 120 min was required to reach

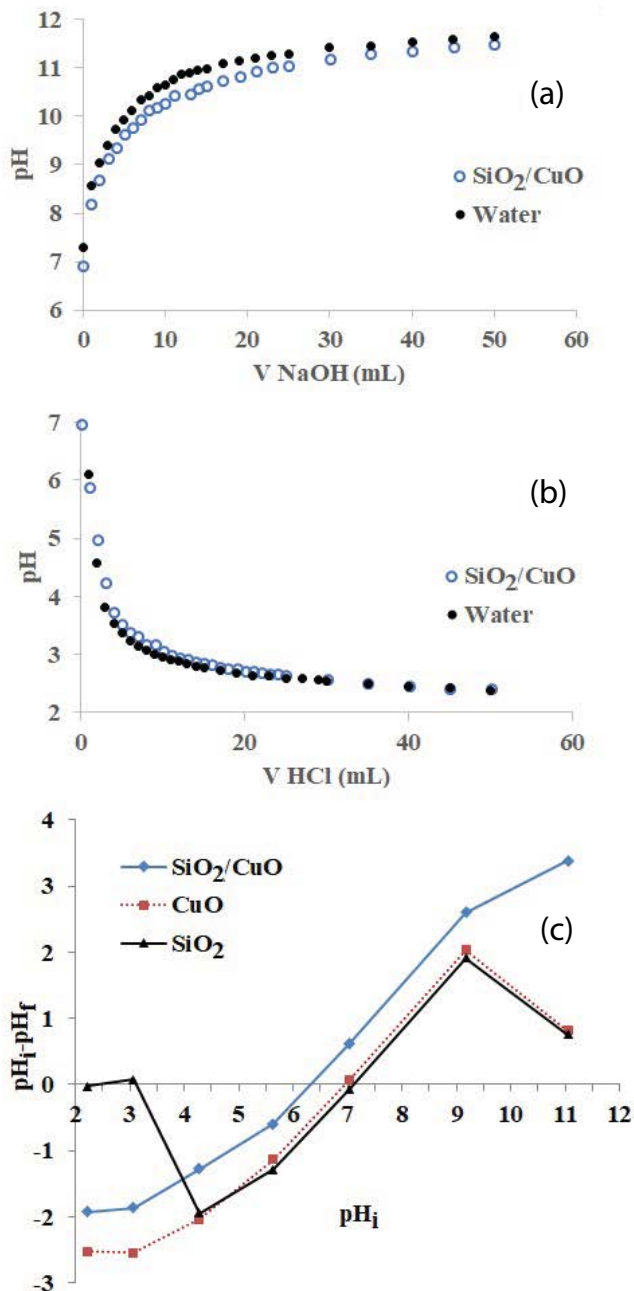


Fig. 5. (a) pH titration curve of SiO₂/CuO with 0.013 M NaOH and HCl. Titration of water was given as a reference. (b) Point of zero charge (pH_{pzc}) of SiO₂/CuO, CuO and SiO₂ determined by the pH drift method.

equilibrium values of 88% and 80%, respectively. On the other hand, negligible amounts of AB and CR (anionic dyes) were adsorbed on SiO₂/CuO during 24 h.

Several models were used to fit the kinetic data, namely, pseudo-first order, pseudo-second order, Weber–Morris intraparticle diffusion and linear film diffusion models. Only pseudo-second order model (Eq. (3)) gave satisfactory fitting with R^2 of 0.9999 and 0.9998 in the case of MB and CV, respectively (Fig. 7). The applicability of pseudo-second order model may indicate that the kinetics of adsorption is

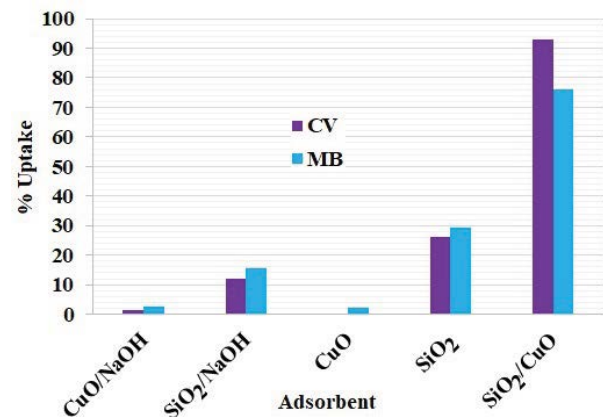


Fig. 6. % uptake (amount adsorbed/initial amount) of methylene blue (MB) and crystal violet (CV) by SiO₂/CuO, precursors (CuO and SiO₂) and alkali-treated precursors ($C_i = 50$ ppm and adsorbent dose = 8.0 g/L).

determined by interaction between the dyes and the surface of SiO₂/CuO rather than by film or intraparticle diffusion processes [29]. The calculated rate constant (k_2) was very high in the case of MB and CV (0.68 and 0.54 g mg⁻¹ min⁻¹, respectively). The high k_2 value may arise from the small particle size of SiO₂/CuO which results in reduced diffusion resistance [29]. The k_2 values obtained in the present work were higher than those reported by other researchers for adsorption of MB on mesoporous silica (0.307 g mg⁻¹ min⁻¹) [4], adsorption of methyl violet 10B dye on alkali activated aluminosilicates (geopolymer) (0.02096 g mg⁻¹ min⁻¹) [16] and adsorption of CV on zeolite A (0.094 g mg⁻¹ min⁻¹) [36]. Chen et al. [43] studied adsorption of Rhodamine B on silica nanoparticles prepared from tetraethoxysilane, cationic surfactant and ammonia. The adsorption process was fast where 90% of the dye was adsorbed in the first 5 min and the pseudo-second order rate constant (k_2) was 0.16 [43].

3.3.4. Adsorption isotherms

The isotherms of adsorption of MB, CV, AB and CR onto SiO₂/CuO are shown in Fig. 8. The data were fitted using nonlinear regression of Langmuir and Freundlich models (Eqs. (4) and (5)) and the results (Table 3) indicated that the adsorption capacity decreases in the following order: CV > MB >> CR > AB. Cationic dyes (CV and MB) were adsorbed more effectively than anionic dyes (CR and AB).

The adsorption capacities of dyes in the present work were lower than those reported by other researchers for adsorption of dyes on carbon, minerals and agricultural wastes (Table 4). This may be since the concentration range used in the present work (5–50 ppm) is much lower than that employed in other studies (up to 1,000 ppm). The adsorption capacity increases as the concentration of the dyes increases because of the more possibility of forming multi-layers of dyes on the surface of adsorbents [44]. We think that the removal of low amounts of dyes from water is not less important than the removal of high concentrations because the latter could be removed by other methods such as coagulation. Regeneration of the composite adsorbent was

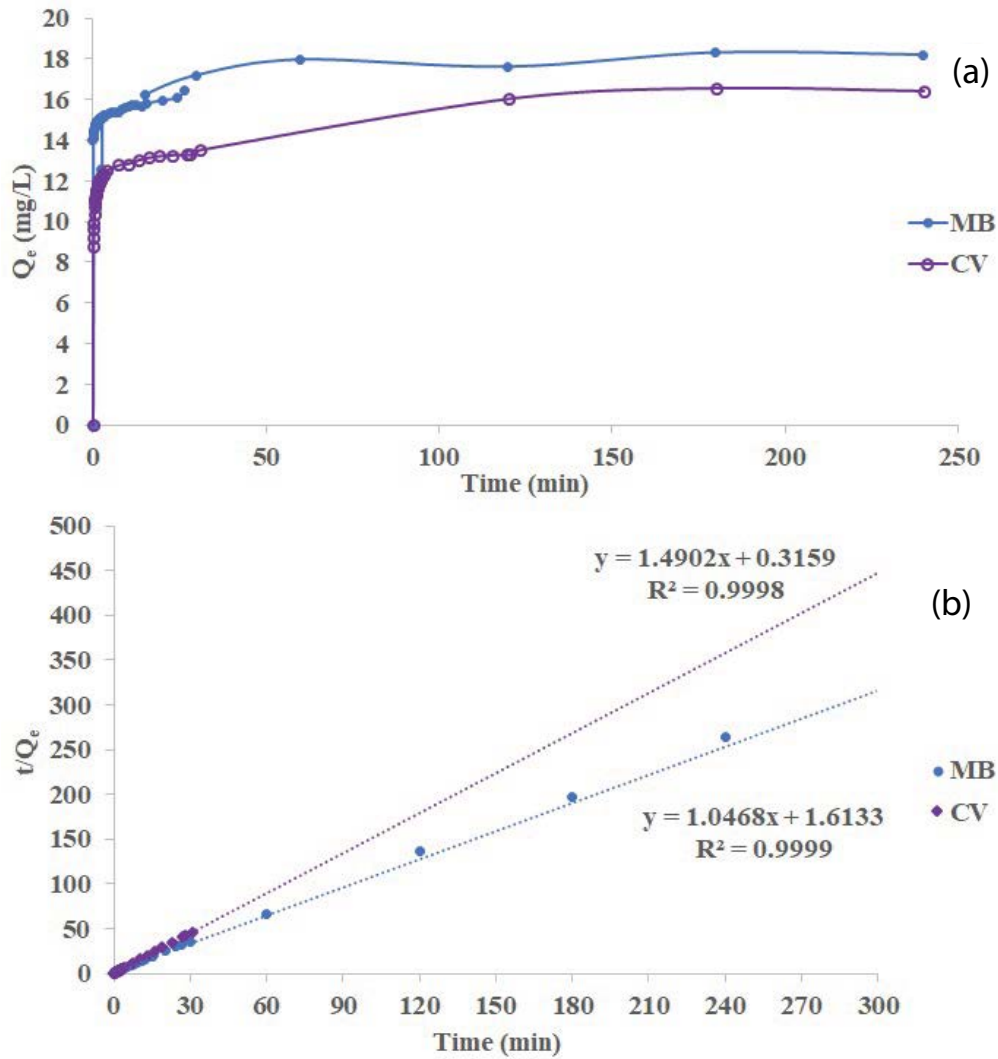


Fig. 7. Effect of contact time on the adsorption of MB and CV on SiO₂/CuO (a), and pseudo-second order fitting of kinetic data for adsorption of MB and CV on SiO₂/CuO (b) ($C_i = 20$ ppm and adsorbent dose = 20 g/L).

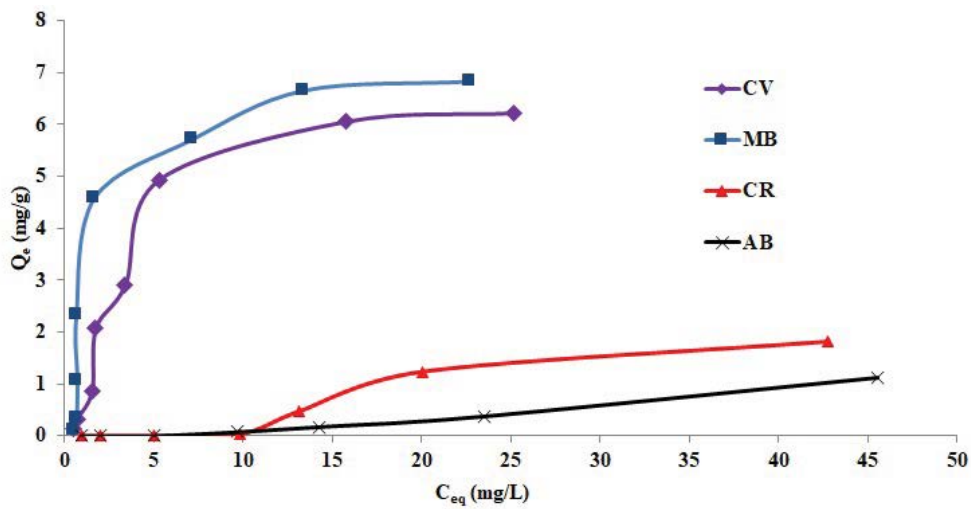


Fig. 8. Isotherms of adsorption of organic dyes (MB, CV, AB, CR) on SiO₂/CuO.

Table 3
Langmuir and Freundlich parameters for adsorption of organic dyes (MB, CV, AB, CR) on SiO₂/CuO (pH = 6.5, dose = 8.0 g/L)

Dye	Q_m (mg/g)	K_L (L/mg)	Error*	K_F	1/n	Error*
MB	7.85	0.390	0.95	2.144	0.41	1.35
CV	8.08	0.175	0.61	1.444	0.49	1.01
AB	1.12	0.0304	0.25	0.002	1.67	0.01
CR	1.52	0.0584	0.48	0.026	1.14	0.26

$$\text{*Standard error} = \sqrt{\frac{\sum (y_i - \hat{y}_i)^2}{n-2}}, y_i: \text{experimental}, \hat{y}_i: \text{predicted.}$$

Table 4
Reported adsorption capacities (mg/g) of MB, CV, AB and CR on different adsorbents

Adsorbent	Category	MB	CV	AB	CR	Reference
AC	Carbon	40–500		550	200	[9]
Coal		250				[41]
Kaolin					1.98	[9]
Bentonite		150–175				[9]
Bentonite	Minerals		370			[11]
Bentonite		1,667				[9]
Red mud		4.3–17			4–7	[13]
Soil clay		31	33			[13]
Synthetic zeolite			11			[15]
Rice husk		312				[45]
Coir pitch					3	[10]
<i>Citrullus lanatus</i> rind			12			[10]
Broad bean peets	Agricultural	193				[10]
Orange peel	waste	33				[18]
Orange peel (calcined 300°C)		14				[18]
Pomelo fruit peel					0.8–1.1	[18]
Grape fruit peel			250			[18]

successfully carried out by dissolution of the dyes loaded onto SiO₂/CuO using ethanol.

3.3.3. Effect of ionic strength

The effect of ionic strength on the adsorption of MB, CV, AB and CR onto SiO₂/CuO is shown in Fig. 9. Increasing the ionic strength was found to decrease the adsorption of cationic dyes (MB and CV) and increase the adsorption of anionic dyes (AB and CR).

Regarding the negative effect of ionic strength on the adsorption of dyes, similar observations were found in the literature in the case of adsorption of basic red 46 (cationic dye) on natural zeolite [14] and adsorption of CV and astrazon red violet (cationic dyes) on bentonite [11]. The positive effect of ionic strength on the adsorption of anionic dyes was also reported in the case of adsorption of reactive yellow 176 (anionic dye) on natural zeolite [14]. Similar effects were reported also for adsorption of CR on bentonite [11] and for adsorption of reactive blue 2, reactive yellow 2 and reactive red 4 (anionic dyes) on activated carbon [12].

The negative effect of ionic strength on the adsorption of cationic dyes was ascribed to the decrease of the thickness

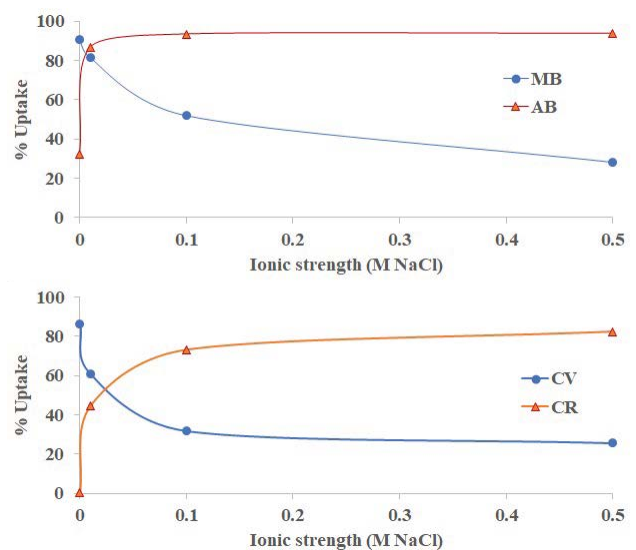


Fig. 9. Effect of ionic strength on the adsorption of MB and AB on SiO₂/CuO.

of the double layer [11,14]. On the other hand, the positive effect of ionic strength on adsorption of anionic dyes was attributed to the aggregation of anionic dyes molecules [14]. The sulfonate group, which is the common group in anionic dyes (in contrast to ammonium group in cationic dyes) may be responsible for this aggregation.

4. Conclusion

SiO₂/CuO can be prepared easily by dissolution of diatomaceous earth (cristobalite, SiO₂) in 6.0 M NaOH followed by deposition on CuO. The composite consists of agglomerates of CuO and amorphous silica. The charge of the surface of the composite (pH_{pzc} = 6.3) is slightly anionic and consequently, it has lower adsorption capacity toward anionic dyes (CR, AB) than cationic dyes (MB, CV). However, increasing the ionic strength significantly increases the adsorption of anionic dyes and decreases the adsorption of cationic dyes. Thus, selective adsorption of organic dyes on SiO₂/CuO can be accomplished by controlling the ionic strength. Another remarkable feature of SiO₂/CuO as adsorbent is that it has an exceptional fast adsorption rate in the case of MB and CV with the possibility of recycling of the adsorbent by retrieving the dyes using ethanol.

References

- [1] J. Zhu, C. Tang, J. Wei, Z. Li, M. Laipan, H. He, X. Liang, Q. Tao, L. Cai, Structural effects on dissolution of silica polymorphs in various solutions, *Inorg. Chim. Acta*, 471 (2018) 57–65.
- [2] C. Tang, J. Zhu, Z. Li, R. Zhu, Q. Zhou, J. Wei, H. He, Q. Tao, Surface chemistry and reactivity of SiO₂ polymorphs: a comparative study on α -quartz and α -cristobalite, *Appl. Surf. Sci.*, 355 (2015) 1161–1167.
- [3] R.K. Iler, *The Chemistry of Silica, Solubility, Polymerization, Colloid and Surface Properties, and Biochemistry*, John Wiley and Sons, New York, 1979.
- [4] W-T. Tsai, K.-J. Hsien, C.-W. Lai, Chemical activation of spent diatomaceous earth by alkaline etching in the preparation of mesoporous adsorbents, *Ind. Eng. Chem. Res.*, 43 (2004) 7513–7520.
- [5] A. Modrzejewska-Sikorska, F. Ciesielczyk, T. Jesionowski, Synthesis and characterization of precipitated CuO-SiO₂ oxide composites, *Pigm. Resin Technol.*, 41 (2012) 71–80.
- [6] H.E. Chalandar, H.R. Ghorbani, H. Attar, S.A. Alavi, Antifungal effect of copper and copper oxide nanoparticles against penicillium on orange fruit, *Biosci. Biotechnol. Res. Asia*, 14 (2017) 279–284.
- [7] A. Azam, A.S. Ahmed, M. Oves, M.S. Khan, A. Memic, Size-dependent antimicrobial properties of CuO nanoparticles against Gram-positive and -negative bacterial strains, *Int. J. Nanomed.*, 7 (2012) 3527–3535.
- [8] A.P. Cano, A.V. Gillado, A.D. Montecillo, M.U. Herrera, Copper sulfate-embedded and copper oxide-embedded filter paper and their antimicrobial properties, *Mater. Chem. Phys.*, 207 (2018) 147–153.
- [9] M.T. Yagub, T.K. Sen, S. Afroze, H.M. Ang, Dye and its removal from aqueous solution by adsorption: a review, *Adv. Colloid Interface*, 209 (2014) 172–184.
- [10] K.S. Bharathi, S.T. Ramesh, Removal of dyes using agricultural waste as low-cost adsorbents: a review, *Appl. Water Sci.*, 3 (2013) 773–790.
- [11] T. Ngulube, J.R. Gumbo, V. Masindi, A. Maity, An update on synthetic dyes adsorption onto clay-based minerals: a state-of-art review, *J. Environ. Manage.*, 191 (2017) 35–57.
- [12] Y.S. Al-Degs, M.I. El-Barghouti, A.H. El-Sheikh, G.M. Walker, Effect of solution pH, ionic strength, and temperature on adsorption behavior of reactive dyes on activated carbon, *Dyes Pigm.*, 77 (2008) 16–23.
- [13] A.A. Adeyemo, I.O. Adeoye, O.S. Bello, Adsorption of dyes using different types of clay: a review, *Appl. Water Sci.*, 7 (2017) 543–568.
- [14] D. Karadag, E. Akgul, S. Tok, F. Erturk, M.A. Kaya, M. Turan, Basic and reactive dye removal using natural and modified zeolites, *J. Chem. Eng. Data*, 52 (2007) 2436–2441.
- [15] Jumaeri, E. Kusumastuti, S.J. Santosa, Sutarno, Adsorption of crystal violet dye using zeolite A synthesized from coal fly ash. *IOP Conf. Series: Mater. Sci. Eng.*, 172 (2017) 1–8.
- [16] T.R. Barbosa, E.L. Foletto, G.L. Dotto, S.L. Jahn, Preparation of mesoporous geopolymer using metakaolin and rice husk ash as synthesis precursors and its use as potential adsorbent to remove organic dye from aqueous solutions, *Ceram. Int.*, 44 (2018) 416–423.
- [17] A.A. Siyal, M.R. Shamsuddin, M.I. Khan, N.E. Rabat, M. Zulfiqar, Z. Man, J. Siame, K.A. Azizli, A review on geopolymers as emerging materials for the adsorption of heavy metals and dyes, *J. Environ. Manage.*, 224 (2018) 327–339.
- [18] I. Anastopoulos, G.Z. Kyzas, Agricultural peels for dye adsorption: A review of recent literature, *J. Mol. Liq.*, 200, Part B (2014) 381–389.
- [19] M.M. Allingham, J.M. Cullen, C.H. Giles, S.K. Jain, J.S. Woods, Adsorption at inorganic surfaces. II. Adsorption of dyes and related compounds by silica, *J. Appl. Chem.*, 8 (1958) 108–116.
- [20] S. Chakrabarti, B.K. Dutta, On the adsorption and diffusion of Methylene Blue in glass fibers, *J. Colloid Interface Sci.*, 286 (2005) 807–811.
- [21] A. Krysztafkiewicz, S. Binkowski, T. Jesionowski, Adsorption of dyes on a silica surface, *Appl. Surf. Sci.*, 199 (2002) 31–39.
- [22] S. Kaneko, Adsorption of several dyes from aqueous solutions on silica-containing complex-oxide gels, *Sep. Sci. Technol.*, 17 (1981) 1499–1510.
- [23] M.N. Asl, N.M. Mahmodi, P. Teymouri, B. Shahmoradi, R. Rezaee, A. Maleki, Adsorption of organic dyes using copper oxide nanoparticles: isotherm and kinetic studies, *Desal. Wat. Treat.*, 57 (2016) 25278–25287.
- [24] R. Raghav, P. Aggarwal, S. Srivastava, Tailoring oxides of copper-Cu₂O and CuO nanoparticles and evaluation of organic dyes degradation, *AIP Conference Proc.*, 1724 (2016) 020078.
- [25] A. Mazumder, R. Rano, Synthesis and characterization of fly ash modified copper oxide (FA/CuO) for photocatalytic degradation of methyl orange dye, *Mater. Today-Proc.*, 5 (2018) 2281–2286.
- [26] M. Fertani-Gmati, K. Brahim, I. Khattech, M. Jemal, Thermochemistry and kinetics of silica dissolution in NaOH solutions: Effect of the alkali concentration, *Thermochim. Acta*, 594 (2014) 58–67.
- [27] A.L. Patterson, The Scherrer formula for X-ray particle size determination, *Phys. Rev.*, 56 (1939) 978–982.
- [28] B.H. Hameed, I.A.W. Tan, A.L. Ahmad, Adsorption isotherm, kinetic modeling and mechanism of 2,4,6-trichlorophenol on coconut husk-based activated carbon, *Chem. Eng. J.*, 144 (2008) 235–244.
- [29] K.L. Tan, B.H. Hameed, Insight into the adsorption kinetics models for the removal of contaminants from aqueous solutions, *J. Taiwan Inst. Chem. Eng.*, 74 (2017) 25–48.
- [30] K.Y. Foo, B.H. Hameed, Insights into the modeling of adsorption isotherm systems, *Chem. Eng. J.*, 156 (2010) 2–10.
- [31] R.B. Langston, E.A. Jenne, NaOH dissolution of some oxide impurities from kaolins, *Clays Clay Miner.*, 12 (1964) 633–647.
- [32] S.K. Zong, W. Wei, Z. Jiang, Z. Yan, J.J. Zhu, J. Xie, Characterization and comparison of uniform hydrophilic/hydrophobic transparent silica aerogel beads: skeleton strength and surface modification, *RSC Adv.*, 68 (2015) 54806–55607.
- [33] Munasir, Triwikantoro, M. Zainuri, Darminto, Synthesis of SiO₂ nanopowders containing quartz and cristobalite phases from silica sands, *Mater. Sci.-Poland*, 33 (2015) 47–55.
- [34] E.R. Lippincott, A. Van Valkenburg, C.E. Weir, E.N. Bunting, Infrared studies on polymorphs of silicon dioxide and germanium dioxide, *J. Res. Nat. Bur. Stand.*, 61 (1958) 61–70.

- [35] X. Su, J. Zhao, X. Zhao, Y. Guo, Y. Zhu, Z. Wang, A facile synthesis of $\text{Cu}_2\text{O}/\text{SiO}_2$ and Cu/SiO_2 core-shell octahedral nanocomposites, *Nanotechnology*, 19 (2008) 1–8.
- [36] J. Jiang, S.-H. Kim, L. Piao, The facile synthesis of Cu@SiO_2 yolk-shell nanoparticles *via* a disproportionation reaction of silica-encapsulated Cu_2O nanoparticle aggregates, *Nanoscale*, 7 (2015) 8299–8303.
- [37] P.K. Raul, S. Senapati, A.K. Sahoo, I.M. Umlong, R.R. Devi, A.J. Thakur, V. Veer, CuO nanorods: a potential and efficient adsorbent in water purification, *RSC Adv.*, 4 (2014) 40580–40587.
- [38] Mineralogy Database. Available at: www.webmineral.com.
- [39] www.saylor.org/site/wpcontent/uploads/2011/06/Ionic-Radius.pdf.
- [40] R. Palanivelu, P. Manivasakan, N.R. Dhineshabu, V. Rajendran, Comparative study on isolation and characterization of amorphous silica nanoparticles from different grades of rice hulls, *Synth. React. Inorg. Met. Org. Chem.*, 46 (2016) 445–452.
- [41] S. Sompech, T. Dasri, S. Thaomola, Preparation and characterization of amorphous silica and calcium oxide from agricultural wastes, *Orient. J. Chem.*, 32 (2016) 1923–1928.
- [42] P. Deshmukh, J. Bhatt, D. Peshwe, S. Pathak, Determination of silica activity index and XRD, SEM and EDS studies of amorphous SiO_2 extracted from rice husk ash, *Trans. Indian Inst. Met.*, 65 (2012) 63–68.
- [43] J. Chen, Y. Sheng, Y. Song, M. Chang, X. Zhang, L. Cui, D. Meng, H. Zhu, Z. Shi, H. Zou, Multimorphology mesoporous silica nanoparticles for dye adsorption and multicolor luminescence applications, *ACS Sustain. Chem. Eng.*, 6 (2018) 3533–3545.
- [44] P. Hadi, J. Guo, J. Barford, G. McKay, Multilayer dye adsorption in activated carbons—facile approach to exploit vacant sites and interlayer charge interaction, *Environ. Sci. Technol.*, 50 (2016) 5041–5049.
- [45] V.K. Gupta, Suhas, Application of low-cost adsorbents for dye removal – a review, *J. Environ. Manage.*, 90 (2009) 2313–2342.